Supporting Information

Surface Modification of Adamantane-Terminated Gold Nanoclusters Using Cyclodextrins

Chunyang Yan,[a,b] Chao Liu,[*b] Hadi Abroshan,[c] Zhimin Li,[b] Renhua Qiu,[*a] and Gao Li[*b]

[a] State Key Laboratory of Chemo/Biosensing and Chemometrics, College of Chemistry and Chemical Engineering, Hunan University, Changsha 410000, China.

[b]Gold Catalysis Research Centre, State Key Laboratory of Catalysis, Dalian Institute of Chemical Physics, Chinese Academy of Sciences, Dalian 116023, P. R. China.

[c] Department of Chemistry, Carnegie Mellon University, Pittsburgh, PA 15213, United States.

Email: renhuaqiu@hnu.edu.cn, chaoliu@dicp.ac.cn, gaoli@dicp.ac.cn

Content

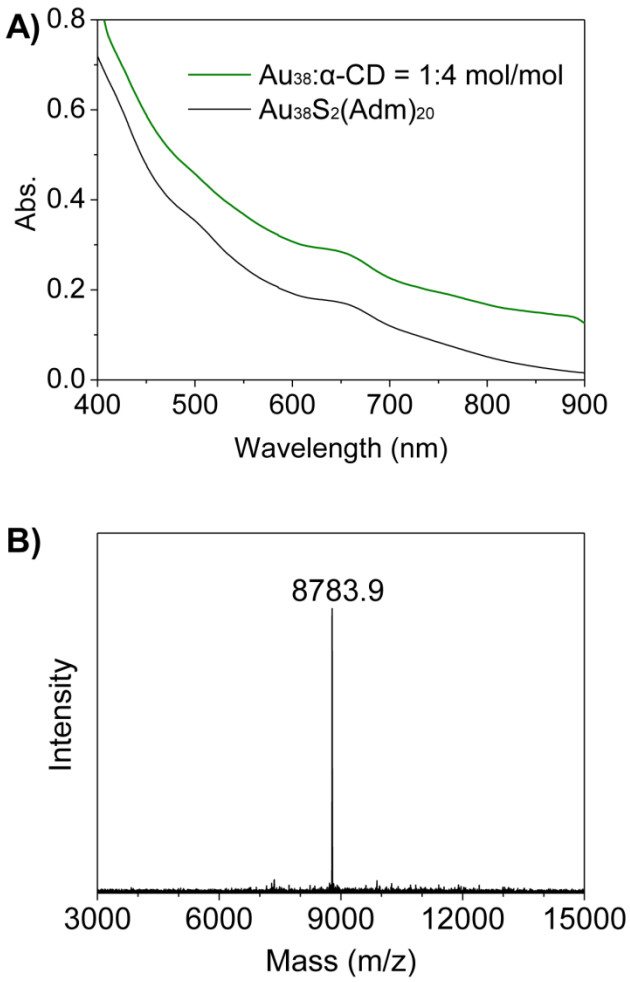

Figure S1. (A) UV-vis of free $Au_{38}S_2(SAdm)_{20}$ nanoclusters and $Au_{38}S_2(SAdm)_{20}$ in the presence of α–CD ($Au_{38}S_2(SAdm)_{20}$:α–CD =1:4, mol/mol). (B) Positive-mode MALDI mass spectrum of $Au_{38}S_2(SAdm)_{20}$ in the presence of α–CD. Of note, the laser intensity is same with that in Figure 1B.

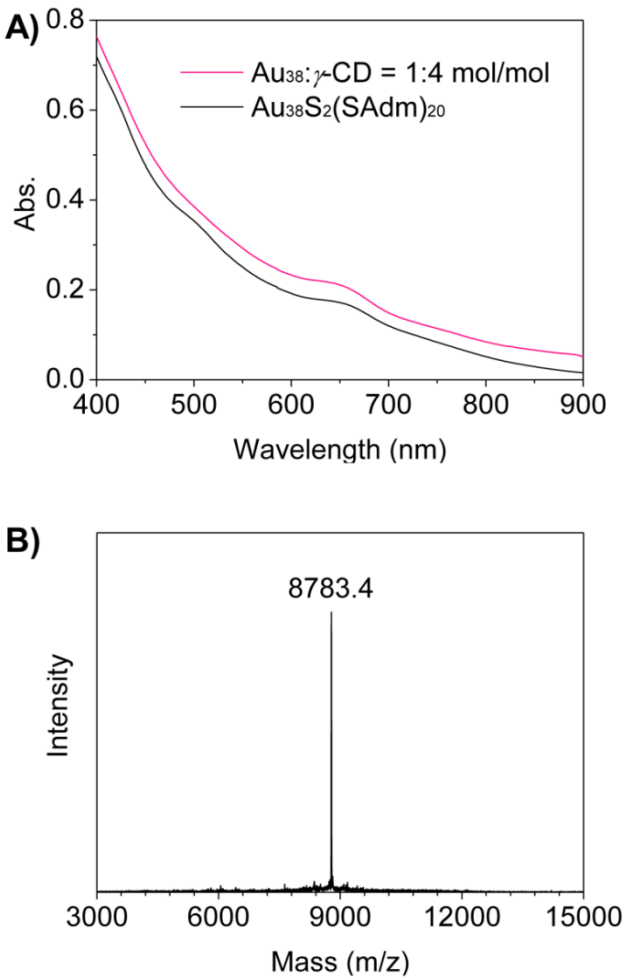

Figure S2. (A) UV-vis of free $Au_{38}S_2(SAdm)_{20}$ nanoclusters and $Au_{38}S_2(SAdm)_{20}$ in the presence of γ–CD ($Au_{38}S_2(SAdm)_{20}$:γ–CD = 1:4, mol/mol). (B) Positive-mode MALDI mass spectrum of $Au_{38}S_2(SAdm)_{20}$ in the presence of γ–CD. Of note, the laser intensity is same with that in Figure 1B.

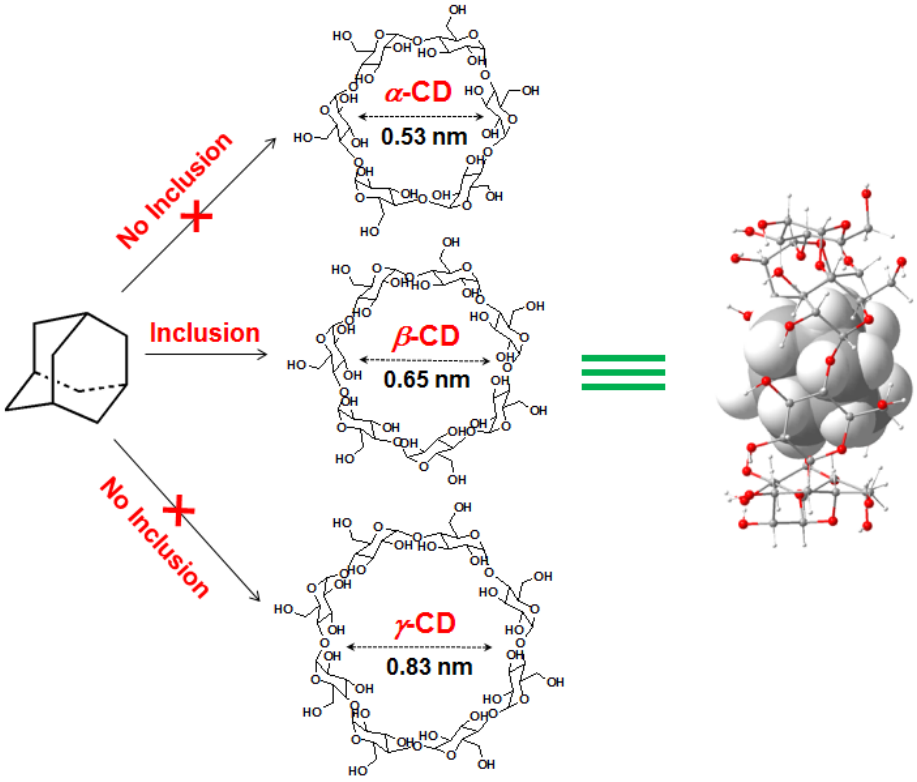

Scheme S1. Illustrations of the inclusion of adamantine group into the cavity of *β*-cyclodextrin (*β*-CD).

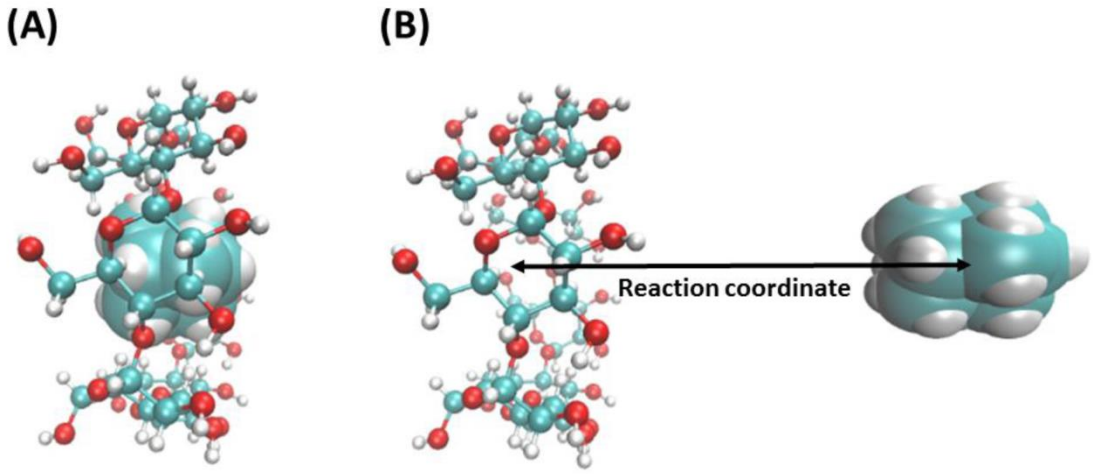

Figure S3. Path between two states of a system: (A) an adamantine occupies the cavity of a cyclodextrin and (B) the adamantine is relatively far away from the cyclodextrin. Of note, distance between centers of adamantine and cyclodextrin molecules is considered as the reaction coordinate.

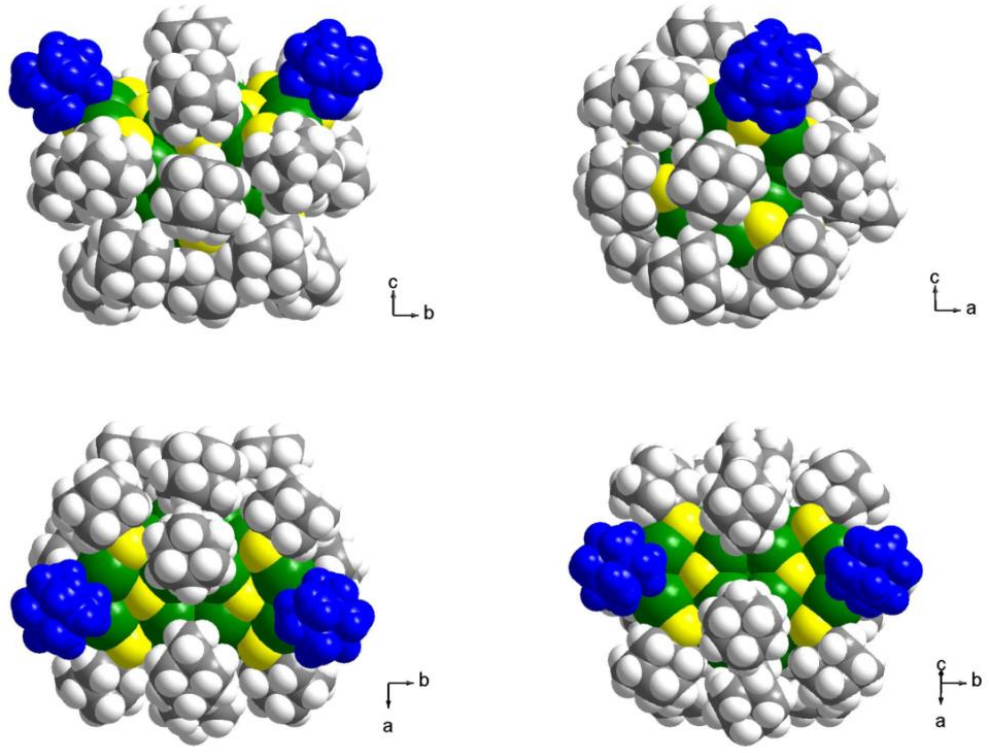

Figure S4. The view of the $Au_{38}S_2(SAdm)_{20}$ nanoclusters along different direction. Two adamantanethiolate ligands are colored in blue.

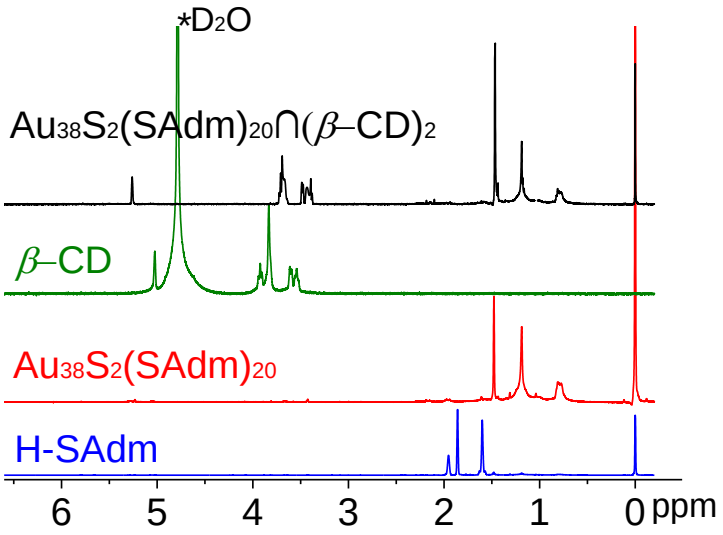

Figure S5. ^{1}H NMR spectra (-0.2 to 6.8 ppm range) of the β–cyclodextrin, adamantanethiol ligand (H-SAdm), unmodified $Au_{38}S_2(SAdm)_{20}$ nanoclusters and $Au_{38}S_2(SAdm)_{20}$-(β–CD)$_2$ conjugates. ^{1}H NMR peaks of free H-SAdm locate at 1.95, 1.84, and 1.60 ppm. The ^{1}H NMR peaks of $Au_{38}S_2(SAdm)_{20}$ nanocluster are red-shifted to 1.47, 1.18, and 0.79 ppm, implying that –SAdm ligands are attached to the surface gold atoms. Such compared to the free β–cyclodextrin, the NMR signal also shifts (Figure S4), indicating that the β–cyclodextrin molecules trap on the –SAdm ligand.

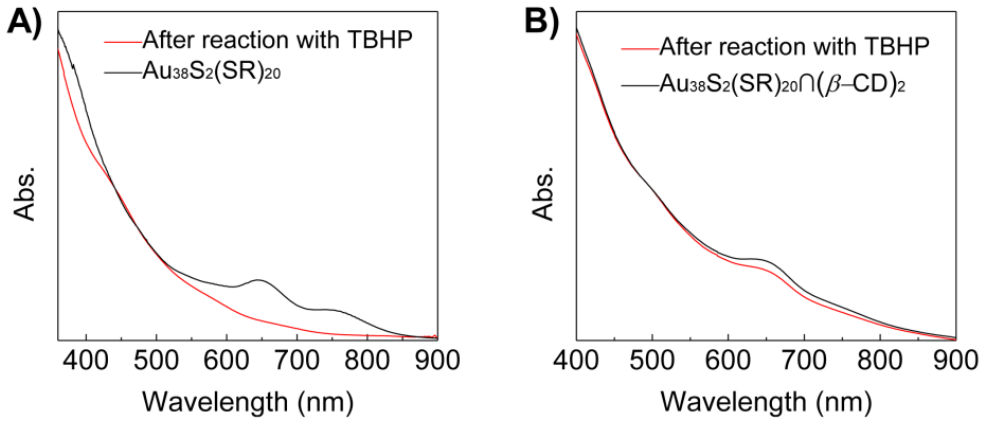

Figure S6. Anti-oxidation properties of (A) $Au_{38}S_2(SAdm)_{20}$ nanoclusters and (B) $Au_{38}S_2(SAdm)_{20}$-(β–CD)$_2$ conjugates in the presence of TBHP oxidant (test conditions: ca. 0.1 mmol $Au_{38}S_2(SAdm)_{20}$ nanoclusters or $Au_{38}S_2(SAdm)_{20}$-(β–CD)$_2$ conjugates were dissolved in THF, 2 mmol TBHP, for 10 h at room temperature).

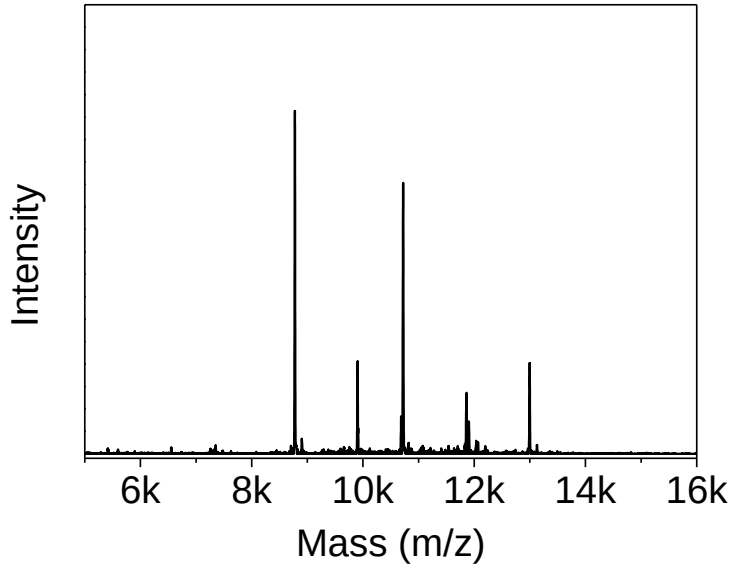

Figure S7. MALDI mass spectrum of $Au_{38}S_2(SAdm)_{20}$-(β–CD)$_2$ after treatment with TBHP. Of note, the laser intensity is the same with that in Figure 2B.

MALDI-MS analysis of the $Au_{38}S_2(SAdm)_{20}$ nanoclusters after the treatment with TBHP was also performed. No mass peaks in m/z > 1000 are found, indicating the nanoclusters are decomposed to small species.

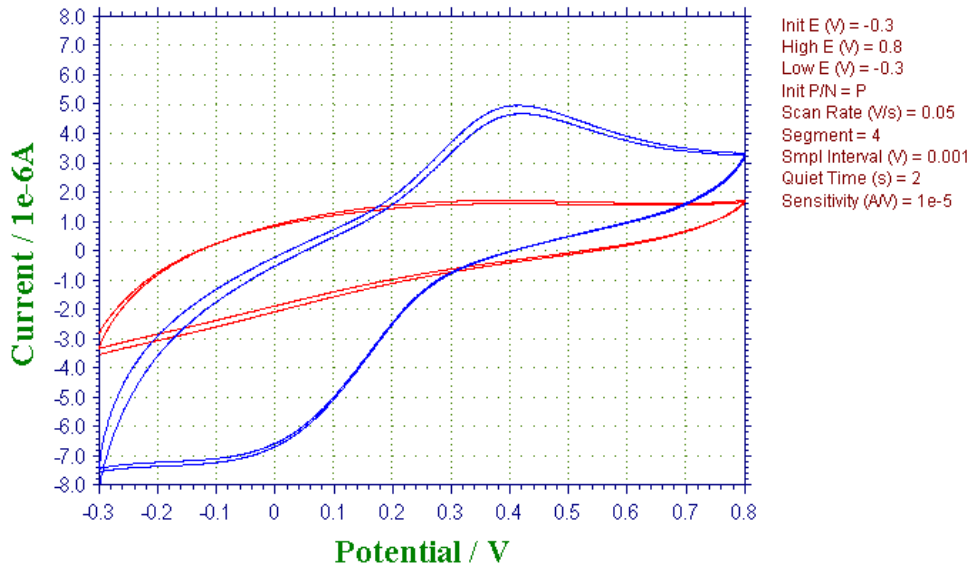

Figure S8. Cyclic voltammograms for the redox reaction in phosphate buffered saline containing potassium ferricyanide on $Au_{38}S_2(SAdm)_{20}$ nanoclusters (blue line) and $Au_{38}S_2(SAdm)_{20}$-(β–CD)$_2$ conjugates (red line).